Melt Rheology of Dendritically Branched Polystyrenes

John R. Dorgan,*,† Daniel M. Knauss,‡ Hasan A. Al-Muallem,‡ and Tianzi Huang‡

Departments of Chemical Engineering and Chemistry, Colorado School of Mines, Golden, Colorado 80401

Dimitris Vlassopoulos

Foundation for Research and Technology−Hellas (F.O.R.T.H.), Institute of Electronic Structure and Laser, Heraklion 71110, Crete, Greece

Received April 19, 2002; Revised Manuscript Received November 14, 2002

ABSTRACT: Unique rheological properties of combined low melt viscosity and high melt elasticity are reported for a novel series of dendritically branched polystyrenes. Unlike previous studies, dendritically branched materials having different molecular weights but all possessing the same number of generations are studied; this allows the determination of true scaling relationships. Zero shear viscosities scale with the second power of molecular weight until corrected to a state of constant free volume, upon which they scale with the first power of molecular weight. Importantly, the steady state shear compliance for the materials increases with increasing molecular weight and is very large compared to other chain architectures. This finding holds potential technological importance as it may be possible to simultaneously decrease viscosity and increase elasticity by blending with these novel structures. Dynamic light scattering and small-angle neutron scattering studies demonstrate the self-similar nature of these highly branched polymers, thereby establishing that the chain architecture is well-defined. Evidence of entanglements is missing. Remarkably, this implies that it is possible to prepare unentangled polystyrenes having a molecular weight in excess of 1 000 000 (g/mol). Melt dynamics are complex; exhibited behavior encompasses aspects of both classical Rouse−Zimm response and the power-law behavior associated with fractal or gelling systems. Neither Rouse−Zimm nor power-law relaxation time distributions are capable of quantitatively describing the data. However, the corrected viscosity scaling and the viscosity shear thinning behavior are in rough agreement with a theory of polymeric fractals proposed by Muthukumar [*J. Chem. Phys.* **1985**, *83,* 3161].

I. Introduction

Architectural variation in the molecular structure of polymer molecules profoundly alters the observed chain dynamics. Understanding and predicting the full spectrum of effects associated with arbitrary branching structure and mixtures of differing architectures remains a challenging problem in polymer physics. In addition, understanding branching and blending has clear commercial significance in terms of adjusting rheological properties to facilitate plastics processing.

Much attention has been paid to understanding the effects of long chain branching. This effort includes both theoretical and experimental studies of well-defined star molecules.[1] In such molecules, arm retraction can be the dominant (i.e., slowest) relaxation mechanism, but whole molecule structural relaxation is also possible. Recently, many groups have sought to understand the effects of relatively sparse long chain branching (LCB).[2−4] A notable theoretical advance in the area is the "pom-pom" model of McLeish and Larson and its derivatives.[5] In these models, the hierarchical relaxation mechanisms are well separated and can be treated in a rigorous manner. Comparison with experiment shows good agreement for the H class of polymer architecture.[6] The state-of-the-art understanding of entangled branched polymer dynamics is now well advanced.[7] The approach, suitable for well-separated time scales, has been extended to the so-called Cayley tree architecture in which every chain segment branches with a fixed functionality at each of its ends.[8] Previous theoretical considerations treated the dynamics of highly branched entangled clusters as might be found in a cross-linking system below the gel point.[9] In all of these studies, the dynamics of entangled polymer strands are treated in accordance with the long chain nature of the branched segments.

In the present investigation, structures having relatively short chain segments (below the entanglement molecular weight) but reasonably large molecular weights (up to 1 million g/mol) are of interest. This combination of molecular features is only achievable through the creation of a highly branched or hyperbranched polymer architectures. In most highly branched polymers, the specific nature of the branching is not well controlled but is rather statistical in nature. In addition, the molecular weight distribution can be broad. As a result, careful experimental studies on the melt viscosity of hyperbranched polymer systems that overcome these problems are not common.[10−13]

Theoretical considerations for unentangled polymers of arbitrary branching structure are available which treat such structures as fractals; specific predictions for rheological functions are provided.[14,15] Fractal dimensions for hyperbranched poly(esteramide)s have been extracted from light and neutron scattering experiments.[16] The state of theoretical understanding for the intermediate regime between entangled polymers and noninterpenetrating colloids remains less developed. Dendritically branched polymers and certain hyperbranched polymers should fall within this regime and

† Chemical Engineering Department.
‡ Chemistry Department.
* To whom correspondence should be addressed. E-mail: jdorgan@mines.edu.

10.1021/ma020612z CCC: $25.00
Published on Web 01/01/2003

Table 1. Structural Characteristics of Dendritically Branched Polystyrenes

sample	ratio of monomer to branching agent	M_w (kg/mol)	M_w/M_n	T_g (°C)	$[\eta]$ in THF at 30 (°C) (dL/g)	average generation no.
C5	5	70.0	1.13	89	0.10	4.5
C10	10	95.0	1.17	90	0.11	4.8
C20	20	213.0	1.21	91	0.16	5.6
C50	50	320.0	1.27	96	0.24	5.3
C92	92	740.1	1.38	99	0.41	5.6
C137	137	862.8	1.45	104	0.52	5.2
C200	200	1313.0	1.81	105	0.96	5.1

offer a number of interesting opportunities for scientific inquiry that have only begun to be explored.

Recently, a study appeared in which a hyperbranched PMMA was carefully fractionated into separate narrow molecular weight distributions.[13] In this system, the dynamic moduli G' and G'' were found to be nearly equal over several decades of frequency, and the complex viscosity fell with a power law exponent of -0.54. This behavior was attributed to the existence of a broad spectrum of relaxation times presumably representing broadness in either the internal branching structure or molecular weights of the size fractionated molecules. The results were taken to be suggestive of gel-like systems beneath the percolation threshold.[17,18] It should be kept in mind though that similar behavior has been reported in highly branched comb polymers for which the branching structure is carefully controlled and homogeneous.[19−22]

Another recent study explores the rheology of a series of hyperbranched polyisobutylenes.[23] Interestingly, the primary dependence of the viscoelastic properties (viscosity and length of the rubbery plateau) is found to rely on the branching frequency (the number of branch strands) rather than the length of the branches. This counterintuitive finding points to the importance of the molecular weight between branch points. In addition, it was found that the zero shear viscosity scales reasonably well with total molecular weight, indicating the importance of molecular size.

Polystyrene microgels represent a type of hyperbranched architecture that in many ways are colloidal in nature; certainly the experimental evidence argues for a lack of entanglements.[10,24] It has been found, however, that linear polystyrene chains can penetrate the microgels when the latter are not too densely cross-linked.[25] This finding leaves open the issue of whether lightly cross-linked microgels can interpenetrate and entangle.

In this paper, the rheological properties of a series of novel, dendritically branched polystyrenes are reported and analyzed. The synthesis of these polymers is conducted using a well-controlled anionic polymerization method based on the convergent technique for synthesizing dendrimers.[26] Unlike most other hyperbranched systems, the polydispersity index for these materials remains relatively low ($p = M_w/M_n \cong 1.3$), and fractionation is not required. In contrast to true dendrimers, the present scheme also allows control of molecular weight in an *independent* fashion from the number of dendritic generations. Accordingly, the structures realized should statistically approach the so-called Cayley tree molecular architecture; a schematic of the expected chain structure is depicted in Figure 1. That is, in the present system the branching frequency is held constant, and the length of the branch strands is systematically varied from 350 to 13 900 g/mol. The present approach allows for careful isolation of the branching, molecular weight, and size contributions to rheological response. For emphasis, the contribution of the present study is that the structure is maintained nearly the same (constant generation), but that the size (molecular weight) is varied. True scaling relationships for dendritically branched polymers having well-controlled structure are presented.

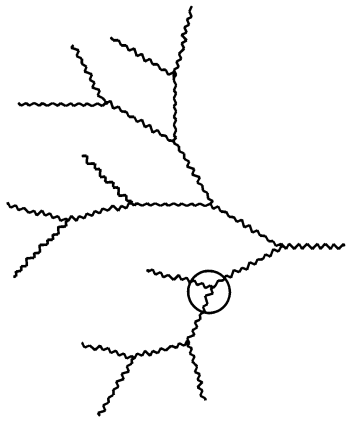

Figure 1. Representative sketch of the anionically prepared dendritic polymers. Some dispersity in the chain lengths between branch points is expected in the materials studied.

II. Materials and Methods

The dendritically branched polystyrenes were synthesized by growing anionic oligomeric living chains and subsequently coupling them in a convergent process along with co-addition of monomer.[26] Absolute weight-average molecular weights were determined using a multiangle laser light scattering (MALLS) detector while distributions were found by gel permeation chromatography (GPC). Details of the anionic polymerization method and materials characterization may be found in ref 26. The properties of the seven different samples, spanning molecular weights from 70 000 to 1 070 000 g/mol, are given in Table 1.

The measurements of the effective hydrodynamic radii (in dilute toluene solutions) were carried out with dynamic light scattering. An ALV goniometer setup and an ADLAS-DPY325 Nd:YAG laser operating at $\lambda = 532$ nm were used. The Brownian motion of the test polymer was detected through the concentration fluctuations of the system at different scattering wavevectors. The equivalent hydrodynamic radius was extracted from the measured diffusion coefficient assuming validity of the Stokes−Einstein relation, $R_H = kT/6\pi\eta D$ (k being the Boltzmann's constant, D the diffusivity, and η the solvent viscosity) for spherical objects.

The radii of gyration, R_G, were estimated from small-angle neutron scattering (SANS) measurements of very dilute solutions in *d*-toluene to extract the form factor. The measurements were carried out at the KWS II, FZ-Juelich, using a neutron wavelength of 6.32 Å, an effective wavelength range from 0.03 to 1.5 nm^{-1}, and three different detector distances. The R_G values reported here were obtained from preliminary Guinier analysis. A complete investigation of the solution properties using SANS, light scattering, and rheology is discussed elsewhere (Asteriadi, A.; Sigel, R.; Vlassopoulos, D.; Meier, G.; Dorgan, J.; Knauss, D., manuscript in preparation).

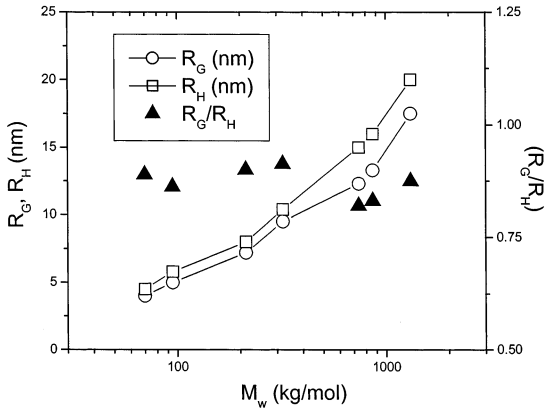

Figure 2. Measured radii of gyrations and hydrodynamic radii vs weight-averaged molecular weight in a series of dendritically branched molecules all of roughly 5 generations. The near constant ratio of R_g/R_h implies a high degree of self-similarity in the branching structure of the materials.

Samples were prepared for melt testing by vacuum molding. The powder sample was placed on a freshly cleaned 25 mm diameter aluminum disk and placed in a vacuum oven at temperatures between 120 and 160 °C. The sample was allowed to flow under the action of gravity until all gas bubbles escaped; no external pressure was applied. The consolidated polystyrene was easily liberated from the aluminum disk but typically fractured into several smaller samples. The recovered pieces were large enough to allow their use for a single dynamic rheology experiment in a parallel plate geometry using a plate diameter of 8 mm. For dynamic experiments employing 25 mm diameter plates, the fractured pieces were reassembled on the test fixture and annealed together. In all cases it was possible to produce a clear, void-free sample of the melt.

Dynamic spectra were obtained on a Rheometrics ARES 2KFRTN1 rheometer in the parallel plate geometry. Diameters of 8 or 25 mm were used along with a gap spacing from 0.5 to 1 mm, over a temperature range of 90−180 °C. Dynamic strain sweeps were performed first in order to determine the regime of linear viscoelasticity. Frequency sweeps were then conducted from 100 to 0.1 s^{-1} for each temperature using a sequence of three decade-wide frequency sweeps, each of which used an appropriate strain corresponding to the linear regime. Master curves were constructed using time−temperature superposition.

III. Results

Figure 2 presents the measured hydrodynamic radii, R_H, and the radii of gyration, R_G, as a function of MW for the samples. Also shown in Figure 2 is the ratio of these two radii (R_G/R_H). The value of R_G/R_H for a hard sphere is 0.78, and for a polymer chain the value is 1.86; these values are independent of size and molecular weight, respectively. That is, for so-called self-similar structures, the ratio is constant. For structural characterization, what should be appreciated is that as the ratio of R_G/R_H increases, the intramolecular crowding decreases. That is, this ratio measures the packing of segments within a molecule. This type of analysis has been widely employed by Burchard in the study of branched polymers.[27] For the present materials, the range is very narrow ($0.82 \leq R_G/R_H \leq 0.92$), thereby implying that the molecules are highly self-similar (they maintain constant intramolecular packing densities). Accordingly, the branching is structurally well-defined.

The range of dynamic response is demonstrated in Figures 3−5 which show the dynamic spectra for the lowest (C5), the second highest (C137), and highest (C200) molecular weight samples. Here, each sample is referenced to the corresponding thermally measured glass transition temperatures for the respective sample (see Table 1). Careful inspection of the loss tangent in the region of the glass transition shows some dispersion (shown later in Figure 7). Such an effect is also reported for polystyrene microgels.[24]

Figure 3 presents the results for the sample of lowest molecular weight (C5). With increasing frequency, the dynamic loss modulus, G'', always remains below the

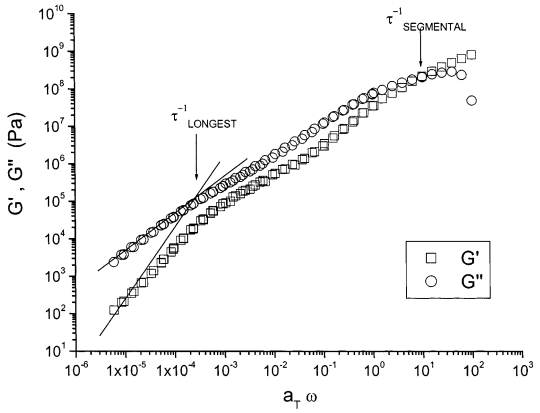

Figure 3. Dynamic spectra for sample C5 referenced to the glass transition temperature. A graphical method for determining the approximate longest and segmental relaxation times is also shown.

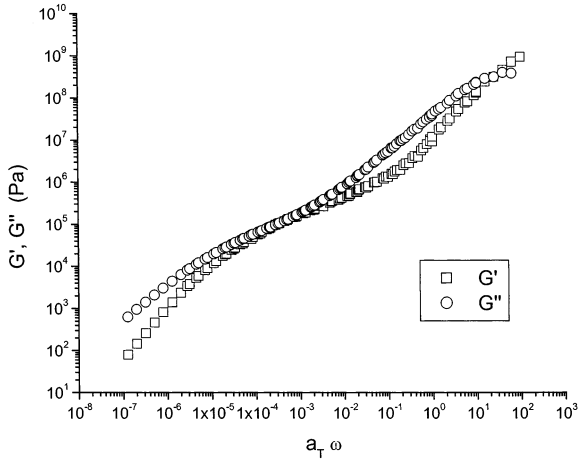

Figure 4. Dynamic spectra for sample C137 referenced to the glass transition temperature.

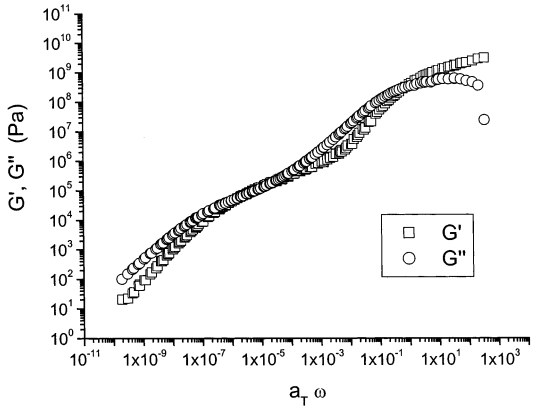

Figure 5. Dynamic spectra for sample C200 referenced to the glass transition temperature exhibiting little evidence of entanglement interactions.

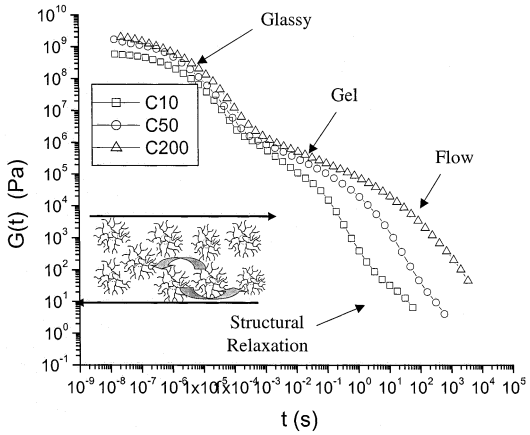

Figure 6. Stress relaxation moduli for samples C10, C50, and C200 demonstrating the widening of the intermediate plateau region with increasing molecular weight. Lower molecular weight samples appear to exhibit some evidence of structural relaxation. The inset shows structural relaxation by whole molecule displacement mechanism.

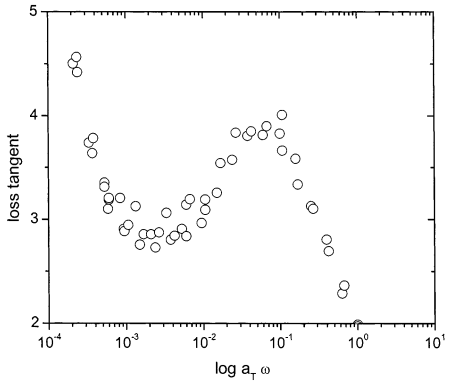

Figure 7. Loss tangent vs reduced frequency in the vicinity of the glass transition showing a loss of time−temperature superposition in this region.

corresponding value for the storage modulus, G', until the glass transition is reached. Such behavior is characteristic of unentangled polymers. Immediately following the terminal regime, G' and G'' rise in a very nearly parallel fashion for more than a decade. The corresponding power-law exponents are 0.77 for G' and 0.73 for G''—that is, they rise roughly with a $^3/_4$ power. Accordingly, the observed behavior is referred to as "Zimm-like" the difference being that in the Zimm model G' remains below G'', and both rise with a power exponent of $^2/_3$ rather than the observed $^3/_4$. A fuller discussion of dynamics is postponed to the Discussion section.

Figure 4 shows the spectra for the C137 sample also referenced to its own glass transition temperature. Here, the behavior is reminiscent of Rouse dynamics for unentangled linear chains. The terminal regime is followed by over a decade in frequency during which G' and G'' lay directly on top of each other; the respective power-law exponents are 0.47 and 0.53. The expected exponent of $^1/_2$ associated with the Rouse model is closely followed, and with the exception of a few scattered points G' systematically remains below G'' throughout the intermediate region. Similar behavior has been reported in other highly branched systems; carefully controlled comb polymers show the same $^1/_2$ exponent[19] while other gel and hyperbranched systems exhibit a lower exponent value of approximately 0.4.[10,13] It should be noted at this point though that Rouse dynamics are not truly observed as will be detailed in the Discussion section.

Table 2. Characteristics of the Observed Power-Law Regions[a]

sample	exponent	decades	sample	exponent	decades
C5	0.75	2.7	C92	0.53	4.5
C10	0.74	2.9	C137	0.50	4.8
C20	0.63	2.6	C200	0.48	5.5
C50	0.57	3.9			

[a] The exponent corresponds to the slope of the dynamic moduli vs frequency while the number of decades refers to the breadth of the intermediate regime in the stress relaxation modulus (see text).

In Figure 5, the dynamic spectra for the highest molecular weight sample, C200, are shown. It should be clear to the reader that there is no definitive evidence of true entanglement dynamics in the data presented. The degree of overlap is suggested as an important dynamic variable in theoretical treatments of polymeric fractals.[9] However, only on the basis of observation of the melt dynamics, it is not possible to make a definitive statement regarding if the structure of these dendritically branched materials allows overlap and interpenetration in the melt state.

The observed behavior for samples having molecular weights intermediate between C5 and C200 follows a systematic trend. As the molecular weight is increased, G' and G'' become less separated and follow a power-law with a decreasing average exponent. This type of power-law stress decay has been attributed to self-similar molecular structures.[18] Equation 1 gives the expression for the stress relaxation modulus,

$$G(t) = St^{-n} \tag{1}$$

where $G(t)$ is the time-dependent modulus, S represents the strength, and n is the decay exponent. A summary of the observed exponents characterizing the power-law region for the various samples is given in Table 2.

Stress relaxation moduli derived from the dynamic data are presented graphically in Figure 6. Careful inspection reveals that the intermediate plateau region increases in width with increasing molecular weight. Another interesting feature in the data of Figure 6 is the existence of a long time inflection in the data for the low molecular weight sample (C10); similar inflections are observed in the data for samples C5 and C20. A slight feature is present in the C50 sample while the higher molecular weights show no such phenomena (C100, C137, and C200); this absence is presumably due to the phenomena being outside of the experimentally observable frequencies. The existence of such a low-frequency secondary relaxation mode may be due to different molecular mechanisms. For example, structural relaxations associated with whole particle movement are observed in highly functionalized star molecules.[28] Arm retraction in H-polymers and other branched architectures can produce similar hierarchical stepwise relaxation phenomena. With the present materials, whole particle movement is a more likely slow mode relaxation mechanism. It should also be appreciated that the phenomena may alternatively be attributable to artifacts associated with measuring very low stresses; in the present study all measurements were within the instrumental range reported by the manufacturer.

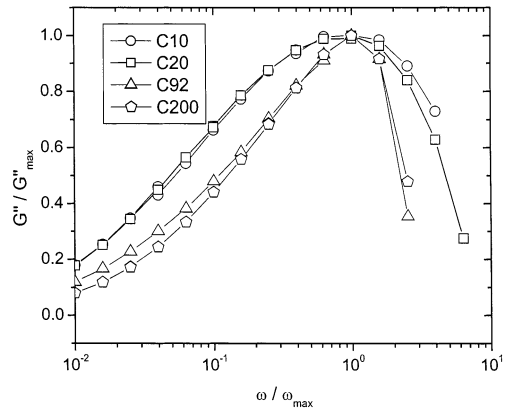

Figure 8. Breadth of the segmental relaxation. As the strand length between branch points decreases, the segmental relaxation broadens, indicating greater cooperativity of motion.

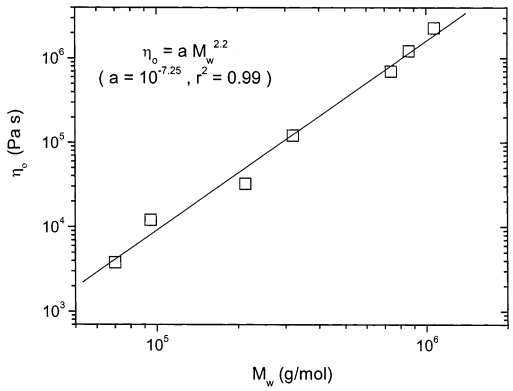

Figure 9. Zero shear viscosity 130 °C vs weight-average molecular weight for dendritically branched polystyrenes of constant generation number. A scaling exponent near 2 is found.

As mentioned above, TTS fails in the region of the glassy transition. That is, the shift factors appropriate for the terminal region produce greater scatter in the shifted data near T_g. This effect is shown in Figure 7 for sample C50.

In cross-linked networks, the breadth of the segmental relaxation is affected by cross-linking density, and this phenomenon has recently been reported for polystyrene microgels.[24] The present hyperbranched system exhibits this same type of behavior as evidenced in Figure 8. Here the loss modulus divided by its maximum value (G''/G''_{max}) is plotted vs the corresponding reduced frequency (ω/ω_{max}) for a series of different molecular weights. For relatively long strand lengths between branch points (C92 and C200), a relatively narrow peak is observed. However, for shorter strand lengths (C10 and C20) the peak is wider. Enhanced cooperativity between segments associated with cross-linking is responsible for this observation.

An unusual finding is presented in Figure 9 which shows the zero shear viscosity plotted vs the total weight-averaged molecular weight at a reference temperature of 130 °C. In the data, G'' has reached its limiting slope value of 1, implying that terminal behavior can be observed according to eq 2.

$$\eta_0 = \lim_{\omega \to 0} \frac{G''(\omega)}{\omega} \tag{2}$$

Furthermore, the zero shear viscosities were determined by fitting the complex viscosity curves to the Carreau−Yasuda model, thus providing an excellent representation of the constant zero shear viscosity value. Rather than the first-order dependence of viscosity on molecular weight expected for unentangled linear chains or the slope near 3.4 found for entangled linear polymers, the scaling exponent is found to be 2.2 ± 0.1. Including or excluding the highest molecular weight material does not influence this slope within the reported uncertainty. A previous report on the rheology of dendritic materials does show an exponent greater than 2 and less than 3; however, considerable scatter exists in the data of that study.[12] Such scatter is not unexpected as the interpretation of such data is complicated because the molecular weight spans different dendrimer generations. No such complication exists in the present data set that more clearly exhibits a scaling power near two.

The scaling of the viscosity with molecular weight in the present dendritic systems can be compared to the previously reported polystyrene microgels.[10] As mentioned above, these gels show a widening of the segmental dispersion with increasing cross-link density. These microgels also show a Zimm-like behavior at low molecular weights, then a crossover of the storage and moduli at larger values, followed finally by a true gel-like response at the highest molecular weights (G' independent of frequency in the low-frequency regime). However, in the present case, larger molecular weights are expected to produce materials that do not gel but are characterized by a hierarchy of relaxation events. Additionally, a 3.4 scaling exponent between the zero shear viscosities and total molecular weight is reported for the microgels, and this is also distinct from the present finding presented in Figure 9.

Because of the large number of chain ends in the present molecules (32 and higher), free volume effects must be carefully considered. The above scaling relationships can be placed on an iso-free-volume basis by utilizing elements of WLF theory. This type of analysis was utilized by Farrington et al. in examining dendritic poly(benzyl ether)s[11] and found to be important by Colby and co-workers in determining the correct linear scaling of low molecular weight polybutadienes.[29] In fact, the low molecular weight data for linear polybutadienes shows a power-law exponent close to 2 prior to being corrected to an iso-free-volume state.

According to WLF theory, the shift factor follows eq 3.

$$\log(a_T) = \log\left(\frac{\eta_T}{\eta_{T_0}}\right) = -\frac{C_1(T - T_0)}{C_2 + (T - T_0)} \tag{3}$$

In eq 3, the shift factor a_T is defined as the ratio of the viscosity at temperature T relative to the viscosity at the reference temperature T_0 and C_1 and C_2 are the WLF fit parameters. Fractional free volumes have been calculated according to

$$f/B = 1/2.3C_1 \tag{4}$$

where f represents the fractional free volume, B is a constant usually taken as unity, and C_1 is the first parameter of the WLF fit. Similarly, the thermal expansion coefficient for the free volume is found from

$$\alpha_f = \frac{B}{2.3C_1C_2} \tag{5}$$

Table 3. WLF Shift Parameters and Calculated Free Volumes

sample	T_g (°C)	C_1	C_2	f/B	α_f	T_0 (°C)	C_1	C_2	f/B	α_f	$(f/B)_{calc}$
C5	89	10.5	44.0	0.041	9.3E−04[a]	130	5.8	85.6	0.075	8.7E−04	0.039
C10	90	10.4	40.5	0.042	1.0E−03	130	6.2	81.1	0.070	8.6E−04	0.035
C20	91	11.4	41.2	0.038	9.2E−04	130	6.5	79.0	0.066	8.4E−04	0.034
C50	96	11.8	45.3	0.037	8.2E−04	130	6.8	71.2	0.064	9.0E−04	0.033
C92	99	11.7	40.8	0.037	9.1E−04	130	7.2	77.9	0.060	7.7E−04	0.036
C137	104	10.7	46.1	0.041	8.9E−04	130	8.2	75.5	0.053	7.0E−04	0.035
C200	105	11.5	48.0	0.038	7.9E−04	130	7.4	72.2	0.059	8.1E−04	0.038

[a] Read as 9.3×10^{-4}.

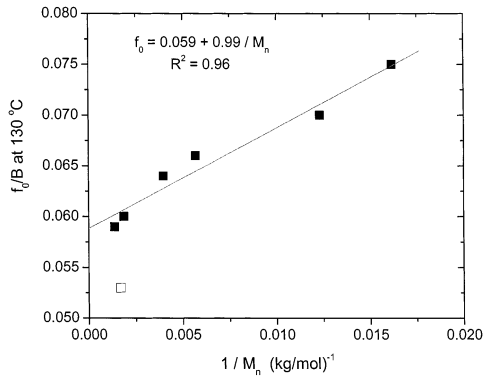

Figure 10. Fractional free volume (f/B) determined from the WLF shift factors corresponding to a reference temperature of 130 °C.

Table 3 summarizes the WLF shift factors for all of the samples referenced to their respective T_g's and to a reference temperature of 130 °C. It is observed that for these materials there is again a relatively constant value of the fractional free volume at T_g of approximately 0.039 ± 0.002. This exceeds the often cited, but not universal, value of 0.025 reported for many linear chain systems.[30] Higher free volume is expected on the basis of the large number of chain ends per molecule, and this effect has been reported for other dendritic systems.[11]

Table 3 also demonstrates that the calculated free volume at the reference temperature of 130 °C follows a systematic trend with T_g—lower T_g materials generally have higher free volumes. However, sample C137 is characterized by an anomalously low f_0/B at the reference temperature; this might be explained by inaccuracies in either the characterization data or shifting parameters. A plot of the fractional free volume against the inverse number-average molecular weight is shown in Figure 10 as suggested by the usual form for the free volume given in eq 6.

$$f_0 = f_\infty + A/M_n \tag{6}$$

In eq 6 f_∞ represents the fractional free volume at infinite molecular weight. A regression of the data (excluding the outlier sample C137) provides a value of 0.059 for f_∞; remarkably, this is near the values reported by both Farrington (for dendrimers) and Colby (for low MW linears).

Because of the consistency in the free volume findings according to WLF theory, the viscosity data of Figure 9 have been corrected to the iso-free-volume condition of for $f_\infty = 0.060$. The correction is accomplished according to eq 7:

$$\eta_0(f_\infty) = \eta_0(f_0)\exp\left(2.3C_1\left(\frac{f_0}{f_\infty} - 1\right)\right) \tag{7}$$

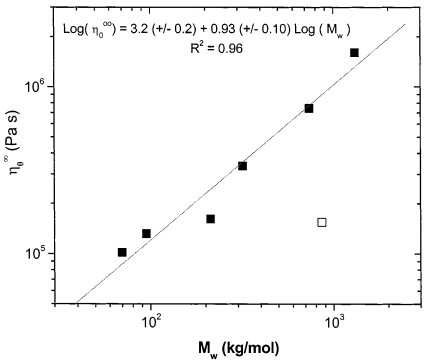

Figure 11. Zero shear viscosities normalized to a constant state of free volume vs weight-average molecular weight at for dendritically branched polystyrenes of constant generation number. A scaling exponent near 1 is found (see text for details).

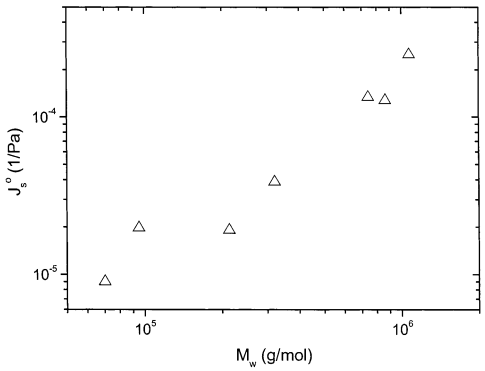

Figure 12. Recoverable shear compliance for dendritic polymers as a function of molecular weight exhibiting a monotonic increase.

Here the f_0 refers to the calculated value at 130 °C. The result of this correction is shown in Figure 11. It is evident that six out of the seven samples now follow a scaling law with an exponent very near unity, the exception being the anomalous sample C137. This finding is very similar to the findings of Colby and coworkers regarding the scaling of low molecular weight linear chains. The appropriate scaling of the viscosity with molecular weight in an important issue in comparing the experimental findings to various theories as discussed below.

In Figure 12 the steady-state compliance ($J_s°$) values are plotted against molecular weight. These values were obtained from the data using eq 7.

$$J_s° = \left(\frac{1}{\eta_0^2}\right)\lim_{\omega\to 0}\left(\frac{G'(\omega)}{\omega^2}\right) \tag{8}$$

To determine the compliance value, a plot of $G'(\omega)/\omega^2$ is made; in this representation numerical values increase as frequency decreases. The low-frequency end

of the data were fit to a single-exponential decay to obtain a value of $G'(\omega)/\omega^2$ that is slightly *lower* than the last few data points (that is, a conservative construction is used that estimates the lower bound of the compliance value), and this value is then divided by the zero shear viscosity squared. Here another characteristic feature of unentangled chains or highly branched materials (like stars for example) is exhibited; the compliance does not plateau but continues to increase with increasing molecular weight. However, the observed values for the dendritics are very large even for a branched structure (see Discussion).

IV. Discussion

The observed features of the present system are unique and represent a novel subclass of hyperbranched polymers with previously unreported rheological properties. The zero shear viscosity scales with an exponent near 2 until corrected for iso-free-volume conditions. This contrasts with previous findings on dendrimers and microgels.[10,11] In stars and other highly branched systems, an exponential dependence on the branch molecular weight or the span molecular weight is found. (The span molecular weight is simply the longest molecular strand, for example, twice the arm length in a star.) This could also be the case for the present hyperbranched materials; the span molecular weight is simply a fraction of the total molecular weight. The natural issue to address is what is the nature of the equilibrium structure and dynamics in these novel hyperbranched molecules? Enthusiasm for the novelty of the findings should be tempered by the fact that the entire data set only spans a decade and a half in molecular weight. Nonetheless, there are a number of clear and important trends that can be observed.

The steady-state compliance presented in Figure 12 warrants comment. As mentioned above, for branched materials, the compliance continues to increase with increasing molecular weight. For monodisperse stars, independent of functionality, the compliance obeys the following expression:

$$J_s^\circ = 0.6\,\frac{M_b}{\rho R T} \tag{9}$$

where M_b is the molecular weight of the branch and ρ is the density in the melt.[31] As mentioned above, the values observed in the dendritic materials are very large. For example, the highest molecular weight dendritic sample has a compliance of 2.5×10^{-4} 1/Pa. In the case of a star architecture, this corresponds to value of M_b of approximately 1.3×10^6 g/mol. This means that at a minimum (functionality, $f = 3$) a star polymer needs a molecular weight of 3.9×10^6 g/mol in order to obtain the same compliance value achieved with a molecular weight of only 1.1×10^6 g/mol in the dendritic architecture! In blends of star polymers with short linear chains (below the entanglement threshold), compliance is reported to follow a simple law of mixtures.[32] Generally, the viscosity of a blend also follows a law of mixtures, and the dendritic viscosities are low. *Accordingly, dendritically hyperbranched materials may prove useful in blends to increase elasticity without incurring a corresponding increase in viscosity*. Studies are underway to explore these potentially important effects.

As mentioned above, the dendritic polymers exhibit some features reminiscent of Rouse−Zimm-like molecular dynamics. In particular, Figures 3−5 demonstrate that G' remains below G'' and that they rise in a very nearly parallel fashion for more than a decade. The dynamics of the Rouse−Zimm model produce the following forms for the dynamic moduli G' and G''

$$G_R'(\omega) = \frac{G'(\omega)}{G} = \sum_i \frac{\omega^2\lambda_i^2}{1+\omega^2\lambda_i^2}$$

$$G_R''(\omega) = \frac{G''(\omega)}{G} = \sum_i \frac{\omega\lambda_i}{1+\omega^2\lambda_i^2} \tag{10}$$

where G_R' represents a reduced modulus, G is the characteristic modulus, and the spectrum of relaxation times, λ_i, are given in terms of a longest relaxation time, λ_1. The spacing of relaxation times in the Rouse model is given by

$$\lambda_i = \lambda_1/i^2 \tag{11}$$

In the Zimm model the only modification to eqs 10 and 11 is in the exponent dictating the spacing of the relaxation times; for a Θ solvent the value is $^3/_2$ while in a good solvent it becomes $^9/_5$. The data of Figures 3−5 as well as dynamic data sets from the other samples cannot be fit to the Rouse and Zimm models with a high degree of success. The fitting is accomplished utilizing a specialized script running under version 6.0 of the Origin software package from Microcal Software; this script calls the built-in Levenburg−Marquet minimization routine in order to provide the best fit model parameters compared to the data sets. In pursuing these calculations, it is revealed that while the data are qualitatively similar to Rouse−Zimm dynamics, quantitatively they are distinct from such descriptions. Likewise, extensions of the bead−spring model to star type of branching are also unable to quantitatively fit the data.[33]

A natural generalization of the Rouse−Zimm type of dynamics is the so-called power-law model in which eq 11 is replaced by

$$\lambda_i = \lambda_1/i^p \tag{12}$$

where p is an exponent that is allowed to float and can be fit to the data. It is perhaps important to realize that a dynamic model comprised of eqs 10 and 12 has the feature of exhibiting a high-frequency response whereby both G' and G'' rise in a parallel fashion according to $\omega^{1/p}$. So the Rouse model rises with $\omega^{1/2}$ while the Zimm model in a good solvent rises with $\omega^{2/3}$. Utilization of the power-law model then encompasses both the Rouse and Zimm models while holding the number of adjustable parameters to 3—the longest time (λ_1), the power exponent (p), and the characteristic modulus (G).

Figures 13 and 14 show the results of fitting the power-law model of eqs 10 and 12 to the lowest molecular weight sample (C5) and highest molecular weight sample (C200), respectively. In these calculations the procedure is to fit the data to the G' data and then calculate the G'' curve utilizing the set of fitted parameter values. In Figure 13, the values determined through the fitting process are $p = 1.37$, $\lambda_1 = 0.06$ s, and $G = 19\,393$ Pa; these values can be compared to those determined assuming that the Zimm model is valid (i.e.,

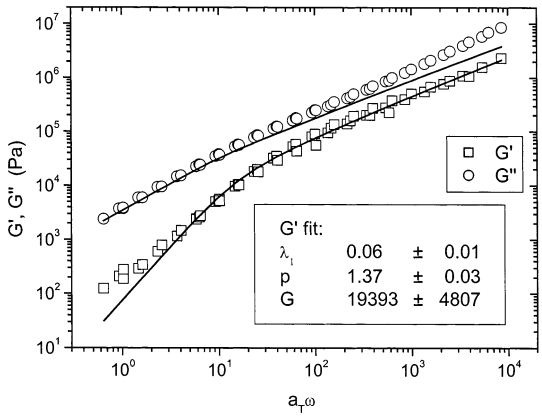

Figure 13. Fit (solid lines) of the data for sample C5 at 130 °C to the power-law dynamics model.

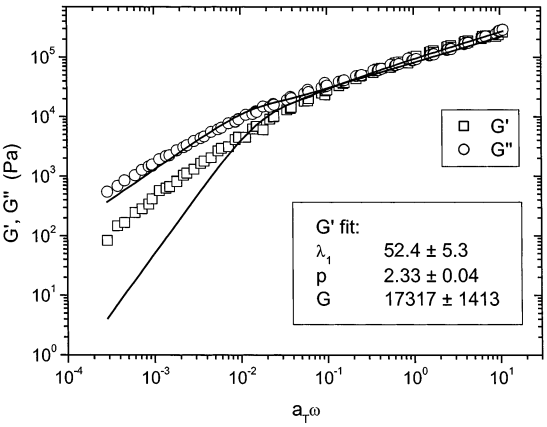

Figure 14. Fit (solid lines) of the data for sample C200 at 130 °C to the power-law dynamics model.

by fixing $p = 1.5$) for $\lambda_1 = 0.02$ s and $G = 48\,200$ Pa. The values determined for sample C200 in the fit shown in Figure 14 are $p = 2.33$, $\lambda_1 = 52.4$ s, and $G = 17\,317$ Pa; the corresponding values for a Rouse model (i.e., by fixing $p = 2.0$) are $\lambda_1 = 78.7$ s and $G = 10\,400$ Pa. The power-law dynamic model does exhibit some self-consistency in that the characteristic modulus for the materials studied falls within a relatively narrow range from 17 to 20 kPa. In addition, power-law relaxation has been associated with gelling and other self-similar systems.[18]

Given the self-similar nature of the dendritic branching evidenced in Figure 2, it is interesting to consider the applicability of theories of polymeric fractals proposed some time ago.[14] Generally, the relationship between mass and size defines the fractal dimension of an object according to eq 13

$$L^{d_f} \sim M \tag{13}$$

where d_f is the fractal dimension. For a solid sphere the fractal dimension is 3 and linear polymers in the melt have a fractal dimension of 2, but if they are dissolved in a good solvent, the fractal dimension falls to $^5/_3$; for a rigid rod of fixed cross section the fractal dimension is 1. In some sense then, the fractal dimension describes the openness of a structure; it measures how much of the mass of an object is accessible at the surface. Figure 15 presents the radii of gyration data vs MW, and it is found that the actual best fit exponent is 0.48; an analysis based on eq 13 gives a corresponding fractal dimension of $d_f = 2.08 \pm 0.08$. A theoretical treatment

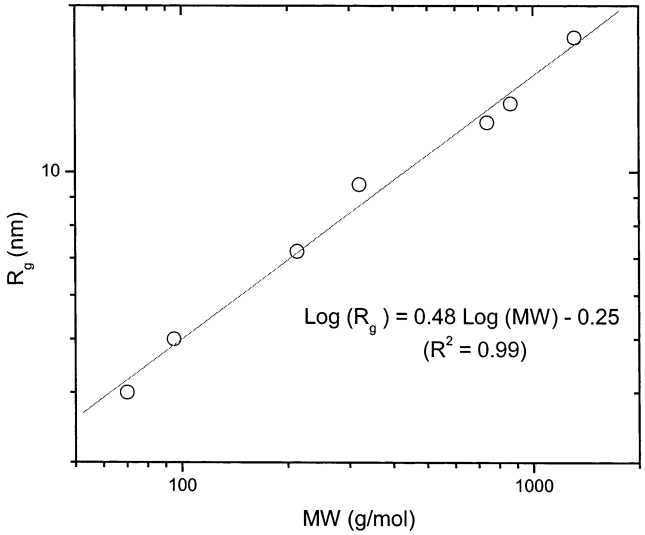

Figure 15. Measured molecular size vs molecular weight. The extracted fractal dimension is 2.08 ± 0.08.

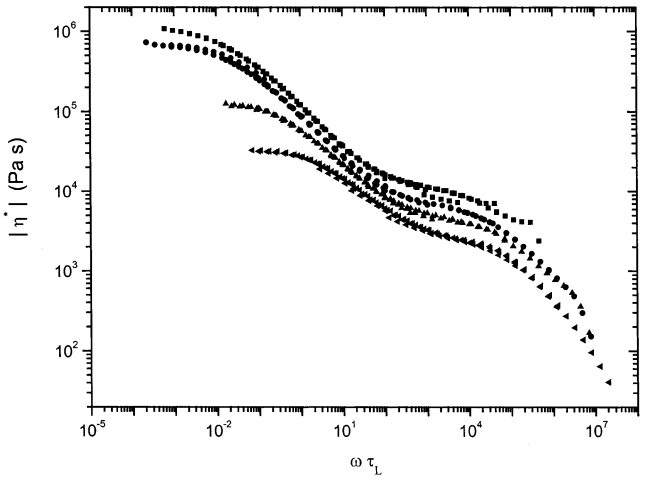

Figure 16. Complex viscosity magnitudes against normalized frequency. The slopes in the intermediate shear-thinning region are around −0.45; this finding is approximately consistent with the fractal theory referenced in the text.

of polymeric fractals predicts a scaling of the zero shear viscosity that follows[14]

$$\eta_0 \sim M^{2/d_f} \tag{14}$$

in which case the free volume corrected data is in approximate agreement with this relationship and the *independently* derived fractal dimension from the radii of gyration data of Figure 15. It should be remembered though that the fractal dimension has been extracted from solution data in which the polymer is under good solvent (toluene) conditions rather than the athermal conditions of the melt. However, this same theoretical treatment also predicts that, in the shear-thinning regime, the viscosity for fractal objects should follow

$$\eta(\omega) = \eta_0 \omega^{-2/(d_f+2)} \tag{15}$$

which provides an additional consistency check. As shown in Figure 16, the shear thinning power exponent is around −0.45; using this value eq 15 yields $d_f = 2.4$. Clearly, there is some inconsistency between the data and the theoretical treatment. (The different predictions

give rough values of $d_f = 2.1$, 2.0, and 2.4.) However, it is also apparent from Figure 16 that not all of the slopes are exactly equal (the range is actually from −0.37 to −0.50, corresponding to fractal dimensions from 2.0 to 3.4). Theoretical considerations could be interpreted to mean that the series of polymers is not truly self-similar but that a different fractal dimension characterizes each sample. However, the data of Figure 2 do indicate a high degree of self-similarity, and the data of Figure 15 provide a value of the fractal dimension near 2. The approximate agreement of eqs 13−15 with the data implies that the fractal treatment does appear to capture some aspects of the dendritically branched materials. To the authors' knowledge, a truly predictive molecular model capable of describing all of the observed viscoelastic response of the present materials is not available.

V. Conclusions

In this study, the unique viscoelastic properties of a novel series of dendritically branched polystyrenes are reported. Unlike previous dendritic materials, the chemistry employed to make the present structures allows independent control over the number of generations and the total polymer molecular weight. The major finding is that combined low melt viscosity and high melt elasticity are possible in dendritically branched polymers. Dynamic light scattering and small-angle neutron scattering studies demonstrate the self-similar nature of these highly branched polymers, indicating that the branching structure is in fact well-defined.

Even the polymers of the highest molecular weight exhibit little indication of entanglement. Remarkably, this implies that it is possible to prepare unentangled polystyrenes having a molecular weight in excess of 1 000 000 g/mol. These and other hyperbranched systems also exhibit some effects that are reminiscent of gel-like behavior. In particular, the parallel scaling of G' and G'' in the intermediate frequency regime resembles the critical gel point in which tan δ becomes independent of frequency. For such gels and other self-similar molecules, a power-law distribution in relaxation times can be invoked but does not quantitatively describe the dynamics.

The observed melt dynamics are complex. Demonstrated behavior encompasses qualitative aspects of both classical Rouse−Zimm response and the power-law behavior associated with gelling or fractal systems. At lower frequencies terminal behavior is reached, and zero shear viscosities follow a first-order power-law dependence on the molecular weight when corrected to a state of constant free volume. Neither Rouse−Zimm nor power-law relaxation time distributions are capable of quantitatively describing the data. However, certain elements of a theory for polymeric fractals do appear to be roughly supported by the available data.

Importantly, the recoverable shear compliance for the materials is found to be anomalously large. This finding holds potential importance for blending as if both viscosity and compliance follow known blending rules, it may be possible to simultaneously decrease viscosity and increase elasticity by blending with these novel structures.

Acknowledgment. The National Science Foundation through the Career Award Program to J.R.D. (CTS-9502466) and D.M.K (DMR-9985221) supported this study. J.R.D. also thanks the F.O.R.T.H institute for hospitality and support during his sabbatical visit that allowed the completion of this work. Acknowledgment is also made to the donors of the Petroleum Research Fund, administered by the ACS, for partial support of this work.

References and Notes

(1) Vlassopoulos, D.; Fytas, G.; Pakula, T.; Roovers, J. *J. Phys. C: Condens. Matter* **2001**, *13*, 855.
(2) Garcia-Franco, C. A.; Srinivas, S.; Lohse, D. J.; Brant, P. *Macromolecules* **2001**, *34*, 3115−3117.
(3) Hatzikiriakos, S. G. *Polym. Eng. Sci.* **2000**, *40*, 2279−2287.
(4) Wood-Adams, P. M.; Dealy, J. M. *Macromolecules* **2000**, *33*, 7481−7488.
(5) McLeish, T. C. B.; Larson, R. G. *J. Rheol.* **1998**, *42*, 81−110.
(6) McLeish, T. C. B.; Allgaier, J.; Bick, D. K.; Bishko, G.; Biswas, P.; Blackwell, R.; Blottiere, B.; Clarke, N.; Gibbs, B.; Groves, D. J.; Hakiki, A.; Heenan, R. K.; Johnson, J. M.; Kant, R.; Read, D. J.; Young, R. N. *Macromolecules* **1999**, *32*, 6734−6758.
(7) McLeish, T. C. B.; Milner, S. T. *Adv. Polym. Sci.* **1998**, *143*, 195−256.
(8) Blackwell, R. J.; Harlen, O. G.; McLeish, T. C. B. *Macromolecules* **2001**, *34*, 2579−2596.
(9) Rubinstein, M.; Zurek, S.; McLeish, T. C. B.; Ball, R. C. *J. Phys. (Paris)* **1990**, *51*, 757−775.
(10) Antonietti, M.; Pakula, T.; Bremser, W. *Macromolecules* **1995**, *28*, 4227−4233.
(11) Farrington, P. J.; Hawker, C. J.; Frechet, J. M.; Mackay, M. E. *Macromolecules* **1998**, *31*, 5043−5050.
(12) Sendijarevic, I.; McHugh, A. J. *Macromolecules* **2000**, *33*, 590−596.
(13) Simon, P. F. W.; Muller, A. H. E.; Pakula, T. *Macromolecules* **2001**, *34*, 1677−1684.
(14) Muthukumar, M. *J. Chem. Phys.* **1985**, *83*, 3161−3168.
(15) Cates, M. E. *J. Phys. (Paris)* **1985**, *46*, 1059−1077.
(16) Gelade, E.; Goderis, B.; de Koster, C. G.; Meijerink, N.; van Nenthem, R. A. T. M. *Macromolecules* **2001**, *34*, 3552−3558.
(17) Winter, H. H.; Mours, M. *Adv. Polym. Sci.* **1997**, *134*, 165−234.
(18) Winter, H. H. *J. Non-Cryst. Solids* **1994**, *172−174*, 1158−1167.
(19) Roovers, J.; Graessley, W. W. *Macromolecules* **1981**, *14*, 766−773.
(20) Vlassopoulos, D.; Fytas, G.; Benoit, H. *Macromolecules* **2000**, *33*, 5960.
(21) Namba, S.; Tsukahara, Y.; Kaeriyama, K.; Okamoto, K.; Takahashi, M. *Polymer* **2000**, *41*, 5165−5171.
(22) Tsukahara, Y.; Namba, S.; Iwasa, J.; Nakano, Y.; Kaeriyama, K.; Takahashi, M. *Macromolecules* **2001**, *34*, 2624−2629.
(23) Robertson, C. G.; Roland, C. M.; Paulo, C.; Puskas, J. E. *J. Rheol.* **2001**, *43*, 759−772.
(24) Roland, C. M.; Santangelo, P. G.; Antonietti, M.; Neese, M. *Macromolecules* **1999**, *32*, 2283−2287.
(25) McGrath, K. J.; Roland, C. M. *Macromolecules* **2000**, *33*, 8354−8360.
(26) Knauss, D. M.; Al-Muallem, H. A.; Huang, T.; Wu, D. T. *Macromolecules* **2000**, *33*, 3557−3568.
(27) Trappe, V.; Burchard, W. Local Dynamics in Branched Polymers. In *Light Scattering and Photon Correlation Spectroscopy*; Pike, E. R., Abbiss, J. B., Eds.; Kluwar Academic Publishers: Dordrecht, The Netherlands, 1997.
(28) Pakula, T.; Vlassopoulos, D.; Fytas, G.; Roovers, J. *Macromolecules* **1998**, *31*, 8931−8940.
(29) Colby, R. H.; Fetters, L. J.; Graessley, W. W. *Macromolecules* **1987**, *20*, 2226−2237.
(30) Ferry, J. D. *Viscoelastic Properties of Polymers*, 3rd ed.; John Wiley & Sons: New York, 1980.
(31) Graessley, W. W. Viscoelasticity and Flow in Polymer Melts and Concentrated Solutions. In *Physical Properties of Polymers*, 2nd ed.; Mark, J. E., Ed.; American Chemical Society: Washington, DC, 1993.
(32) Hadjichristidis, N.; Roovers, J. *Polymer* **1985**, *26*, 1087−1090.
(33) Zimm, B. H.; Kilb, R. W. *J. Polym. Sci.* **1959**, *37*, 19−29.

MA020612Z